Fractals, Vol. 7, No. 3 (1999) 235–247

CONTINUOUS AND DISCRETE MODELS OF COOPERATION IN COMPLEX BACTERIAL COLONIES

I. COHEN*, I. GOLDING, Y. KOZLOVSKY and E. BEN-JACOB
School of Physics & Astronomy,
Raymond & Beverly Sackler Faculty of Exact Sciences,
Tel Aviv University, Tel Aviv 69978, Israel

I. G. RON
Department of Oncology, The Sackler Faculty of Medicine,
Tel Aviv University, Tel Aviv 69978, Israel

Received April 8, 1999; Accepted June 30, 1999

Abstract

In this paper, we study the effect of discreteness on various models for patterning in bacterial colonies (finite-size effect) and present two types of models to describe the growth of the bacterial colonies. The first model presented is the Communicating Walkers model (CWm), a hybrid model composed of both continuous fields and discrete entities — walkers, which are coarse-graining of the bacteria; coarse-graining may amplify the discreteness inherent to the biological system. Models of the second type are systems of reaction diffusion equations, where the branching of the pattern is due to non-constant diffusion coefficient of the bacterial field. The diffusion coefficient represents the effect of self-generated lubrication fluid on the bacterial movement. The representation of bacteria by a density field neglects their discreteness altogether. We implement the discreteness of the bacteria by introducing a cutoff in the growth term at low bacterial densities. We demonstrate that the cutoff does not improve the models in any way. The cutoff affects the dynamics by decreasing the effective surface tension of the front, making it more sensitive to anisotropy and decreasing the fractal dimension of the evolving patterns. We compare the continuous and semi-discrete models by introducing food chemotaxis and repulsive chemotactic signaling into the models. We find that the growth dynamics of the CWm and the growth dynamics of the Non-Linear Diffusion model (one of the continuous models) are affected in the same manner. From such similarities and from the insensitivity of the CWm to implicit anisotropy, we conclude that even the increased discreteness,

*E-mail: inon@albert.tau.ac.il

introduced by the coarse-graining of the walkers, is small enough to be neglected. There are advantages and disadvantages to the two types of models. Employing both of them in parallel enables us to conclude that the discreteness of the bacteria does not significantly affect the growth dynamics (no finite-size effect).

1. INTRODUCTION

The endless array of patterns and shapes in nature has long been a source of joy and wonder to layman and scientists alike.[1–5] During the last decade, there have been exciting developments in the understanding of pattern determination in non-living systems.[4,6–8] The attention of many researchers is now shifting towards living systems, in a hope to use these new insights for the study of pattern forming processes in living systems (see Ref. 9 and references therein). Bacterial colonies offer a suitable subject for such research.[10–22] In some sense, they are similar enough to non-living systems so as their study can benefit from the knowledge about non-living systems, yet their building blocks (bacteria) are complex enough to ensure ever so new surprises.

In Fig. 1, we show representative branching patterns of bacterial colonies. These colonies are made up of about 10^{10} bacteria of the type *Paenibacillus dendritiformis* (see Refs. 23 and 24 for first reference in the literature and Ref. 25 for identification). For other studies of branching bacterial patterns, see Refs. 10, 26–30. Each colony is grown in a standard petri-dish on a thin layer of agar (semi-solid jelly). The bacteria cannot move on the dry surface and cooperatively they produce a layer of lubrication fluid in which they swim (Fig. 2). Bacterial swimming is a random walk-like movement, in which the bacteria propel themselves in nearly straight runs separated by brief tumbling events. The bacteria consume nutrients from the media, nutrients which are given in limited supply. The growth of a colony is limited by the diffusion of nutrients towards the colony — the growth rate of the colony is determined by the bacterial reproduction rate which is limited by the level of nutrients available for the cells. Note that a single isolated bacterium on the agar can reproduce, grow in numbers and make a new colony.

Bacterial colonies entangle entities in many length scales: the colony as a whole is in the range of several centimeters; the individual branches are of width in the range of millimeters and less; the individual bacteria are in the range of micrometers, so is the width of the colony's boundary; and chemicals in the agar such as the constitutes of the nutrient are on the molecular length scale.

Kessler and Levine[31] studied discrete pattern forming systems, using reaction-diffusion models with linear diffusion and various growth terms. It can be showed that the ability of the system to form two-dimensional patterns depend on the

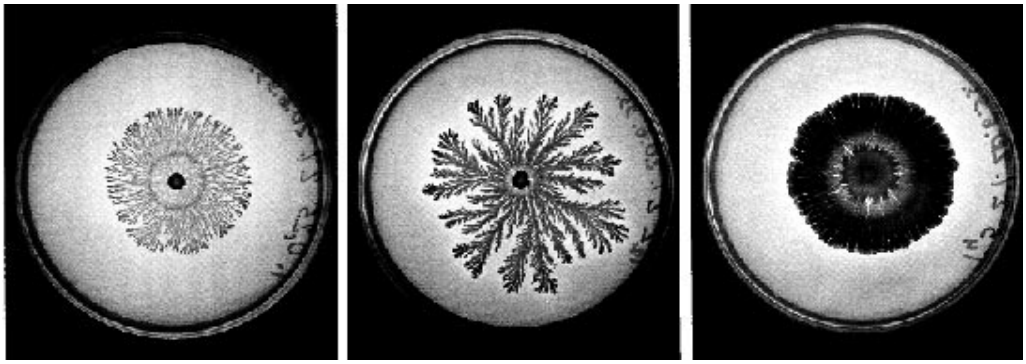

Fig. 1 Observed branching patterns of colonies of *P. dendritiformis* grown on 2% agar concentration. The nutrient level is, from left to right, 0.25 gram peptone per liter, 0.5 g/l and 5 g/l. In the colony on the right, wide branches can be seen, branches much wider than the gaps between them. The pattern in the middle is less ordered, fractal-like pattern, similar to patterns seen in electro-chemical deposition and DLA simulations.[4,8] As the nutrient level is further decreased, the pattern becomes denser again, with pronounced circular envelope (on the left).

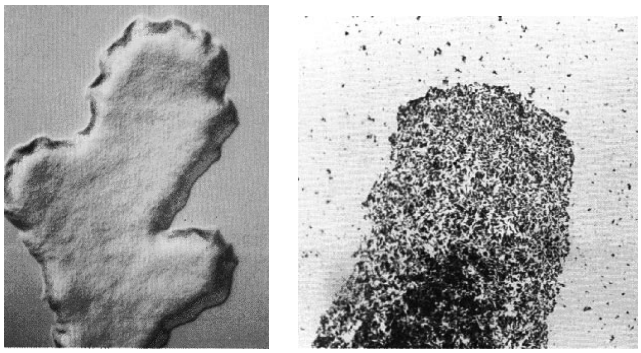

Fig. 2 Closer look on a branch of a bacterial colony. The left figure shows the lubrication fluid in which the bacteria are immersed. On the right, the individual bacteria can be seen. Each dot in the branch is a 1×2 μm bacterium. The dots outside the branch are not bacteria but deformations of the agar.

derivative of the growth term (reaction term) at zero densities. With a negative derivative, the system can form branching patterns; with a positive derivative, the system can form only compact patterns with circular envelope. Kessler and Levine[31] accounted for the discreteness of the system by introducing a low-densities cutoff in the growth term. Doing so to a growth term with positive derivative at zero can introduce bumps to the pattern, which is a manifestation of a diffusive instability in the two-dimensional front (the first step towards a branching pattern).

We present here three models for growth of the bacterial colonies. The first is the Communicating Walkers model (Sec. 2) which includes discrete entities to describe the bacteria, continuous fields to describe chemicals in the agar and an explicit free boundary for the colony's edge. The second model is a continuous one, a reaction-diffusion model that couples the bacterial movement to a field of lubrication fluid (Sec. 3). The diffusion coefficients of the bacterial field and the lubrication field depend on the lubrication fluid, resulting in a spontaneous formation of a sharp boundary (singular line) to the colony. The third model tries to simplify the former model and disposes of the lubrication field by introducing a density-dependent diffusion of the bacterial field (Sec. 4). We discuss the effect of a cutoff in the growth term in the two continuous models. We then turn our attention to various features of the observed bacterial patterns and see similarities in the different models' ability to reproduce these features (Sec. 5).

2. THE COMMUNICATING WALKERS MODEL: A HYBRID MODEL

The Communicating Walkers model (CWm)[11] was inspired by the diffusion-transition scheme used to study solidification from supersaturated solutions.[32–34] The former is a hybridization of the "continuous" and "atomistic" approaches used in the study of non-living systems. The diffusion of the chemicals is handled by solving diffusion equations (including sources and sinks) on a tridiagonal lattice. The bacterial cells are represented by walkers allowing a more detailed description. In a typical experiment, there are 10^9–10^{10} cells in a petri-dish at the end of the growth. Hence, it is impractical to incorporate into the model each and every cell. Instead, each of the walkers represents about 10^4–10^5 cells so that we work with 10^4–10^6 walkers in one numerical "experiment".

The walkers perform an off-lattice random walk on a plane within an envelope representing the boundary of the wetting fluid. This envelope is defined on the same triangular lattice where the diffusion equations are solved. To incorporate the swimming of the bacteria into the model, each of the active walkers (motile and metabolizing, as described below) moves a step of size d at a random angle Θ at each time step. Starting from location $\mathbf{r}_i$, it attempts to move to a new location $\mathbf{r}'_i$ given by:

$$\mathbf{r}'_i = \mathbf{r}_i + d(\cos\Theta, \sin\Theta)\,. \tag{1}$$

If $\mathbf{r}'_i$ is outside the envelope, the walker does not move. A counter on the segment of the envelope which would have been crossed by the movement form $\mathbf{r}_i$ to $\mathbf{r}'_i$ is increased by one. When the segment counter reaches a specified number of hits N_c, the envelope propagates one lattice step and an additional lattice cell is added to the colony. This requirement of N_c hits represents the colony propagation through wetting of unoccupied areas by the bacteria. Note that N_c is related to the agar dryness, as more wetting fluid must be produced (more "collisions" are needed) to push the envelope on a harder substrate.

Motivated by the existence of a maximal growth rate of the bacteria even in optimal conditions, each walker in the model consumes food at a constant rate Ω_c if sufficient food is available. We represent the metabolic state of the ith walker by an "internal energy" E_i. The rate of change of the

internal energy is given by

$$\frac{dE_i}{dt} = \kappa C_{\text{consumed}} - \frac{E_m}{\tau_R} \tag{2}$$

where κ is a conversion factor from food to internal energy ($\kappa \cong 5 \cdot 10^3$ cal/g) and E_m represents the total energy loss for all processes over the reproduction time τ_R, excluding energy loss for cell division. C_{consumed} is $C_{\text{consumed}} \equiv \min(\Omega_C, \Omega'_C)$, where Ω'_C is the maximal rate of food consumption as limited by the locally available food.[9] When sufficient food is available, E_i increases until it reaches a threshold energy. Upon reaching this threshold, the walker divides into two. When a walker is starved for a long interval of time, E_i drops to zero and the walker "freezes". This "freezing" represents the entry into a pre-spore state (starting the process of sporulation, see Sec. 5).

We represent the diffusion of nutrients by solving a diffusion equation for a single agent whose concentration is denoted by $n(\mathbf{r}, t)$:

$$\frac{\partial n}{\partial t} = D_n \nabla^2 C - b C_{\text{consumed}} \tag{3}$$

where the last term includes the consumption of food by the walkers (b is their density). The equation is solved on the tridiagonal lattice. The simulations are started with inoculum of walkers at the center and a uniform distribution of the nutrient.

Results of numerical simulations of the model are shown in Figs. 3 to 5. As in the case of real bacterial colonies, the patterns are compact at high nutrient levels. With decreasing food levels, the patterns become less ordered and their fractal dimension decreases. For a given nutrient level, the patterns are more ramified with decreasing fractal dimension as the agar concentration increases. The results shown in Fig. 3 capture some features of the experimentally observed patterns. However, at this stage the model does not account for some critical features,

Fig. 3 Colonial pattern of CWm. Here $N_c = 20$ and n_0 is 6, 8, 10 and 30 from left to right respectively.

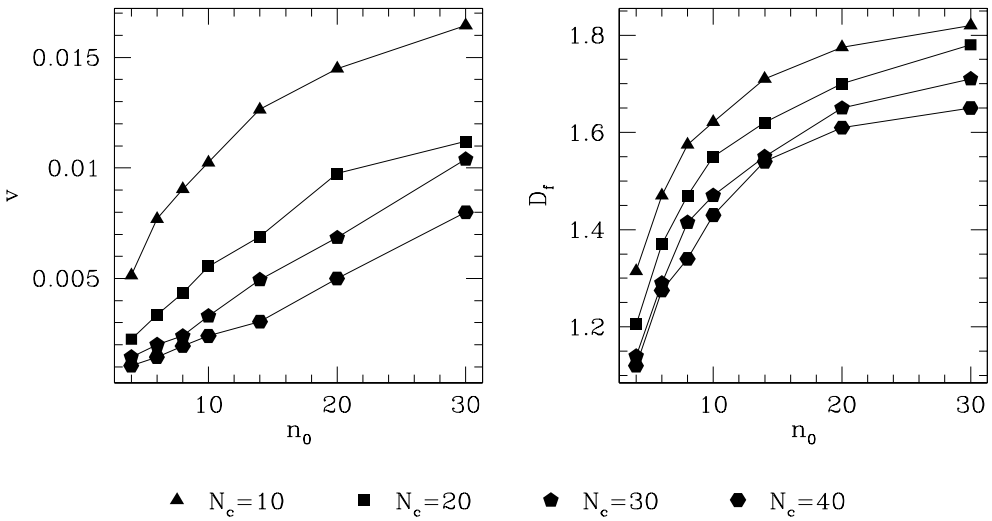

Fig. 4 Fractal dimension and growth velocity as a function of initial food concentrations. The data are for typical runs of CWm. The growth velocity is presented in arbitrary units.

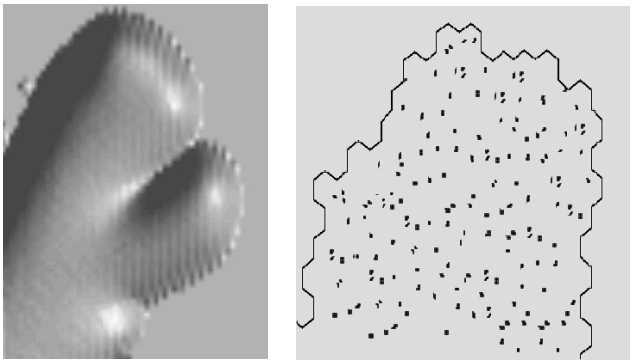

Fig. 5 Closer look on simulated colonies. On the right: a tip of a branch in a run of CWm. The boundary of the branch and walkers can be seen. On the left: lubrication at a tip of a branch in LBm. The boundary of the branch is a singularity line, where the spatial derivative are discontinuous.

such as the ability of the bacteria to develop organized patterns at very low nutrient levels. Ben–Jacob et al.[5,35–37] suggested that chemotactic signaling must be included in the model to produce these features (see Sec. 5).

3. A LAYER OF LUBRICATION

The Lubricating Bacteria model (LBm) is a reaction-diffusion model for the bacterial colonies.[18,19] This model includes four coupled fields. One field describes the bacterial density $b(\mathbf{x}, t)$, the second describes the height of lubrication layer in which the bacteria swim $l(\mathbf{x}, t)$, the third describes the nutrient $n(\mathbf{x}, t)$ and the fourth is the stationary bacteria that "freeze" and begin to sporulate $s(\mathbf{x}, t)$ (see Sec. 5).

The dynamics of the bacterial field b consists of two parts; a diffusion term which is coupled to the lubrication field and represents movement, and a reaction part which is coupled to the nutrient field and contains terms for reproduction and sporulation. Following the same arguments presented for CWm, we get a reaction term of the form $(\kappa b \min(\Omega_C, n) - E_m b/\tau_R)$. Assuming that the nutrient is always the factor limiting the bacterial growth, we get, upon rescaling, the growth term $bn - \mu b$ (μ constant).

We now turn to the bacterial movement. In a uniform layer of liquid, bacterial swimming is a random walk with variable step length and can be approximated by diffusion. The layer of lubrication is not uniform, and its height affects the bacterial movement. An increase in the amount of lubrication decreases the effective friction between the bacteria and the agar surface. The term "friction" is used here in a very loose manner to represent the total effect of any force or process that slows down the bacteria. As the bacterial motion is over-damped, the local speed of the bacteria is proportional to the self-generated propulsion force divided by the friction. It can be shown that variation of the speed leads to variation of the diffusion coefficient, with the diffusion coefficient proportional to the speed to the power of two. We assume that the friction is inversely related to the local lubrication height through some power law: friction$\sim l^{\gamma}$ and $\gamma < 0$. We get an expression for the bacterial flux:

$$\mathbf{J}_b = -D_b l^{-2\gamma} \nabla b \,. \tag{4}$$

The lubrication field l is the local height of the lubrication fluid on the agar surface. Its dynamics is given by:

$$\frac{\partial l}{\partial t} = -\nabla \cdot \mathbf{J}_l + \Gamma b n (l_{\max} - l) - \lambda l \tag{5}$$

where $\mathbf{J}_l$ is the fluid flux (to be discussed), Γ is the production rate and λ is the absorption rate of the fluid by the agar. λ is inversely related to the agar dryness.

The fluid production is assumed to depend on the bacterial density. As the production of lubrication probably demands substantial energy, it also depends on the nutrient's level. We assume the simplest case where the production depends linearly on the concentrations of both the bacteria and the nutrient.

The lubrication fluid flows by diffusion and by convection caused by bacterial motion. A simple description of the convection is that as each bacterium moves, it drags along with it the fluid surrounding it. The diffusion term of the fluid is assumed to depend on the height of the fluid to the power $\eta > 0$ (the nonlinearity in the diffusion of the lubrication, a very complex fluid, is motivated by hydrodynamics of simple fluids):

$$\mathbf{J}_l = -D_l l^{\eta} \nabla l + j \mathbf{J}_b \tag{6}$$

where D_l is a lubrication diffusion constant, $\mathbf{J}_b$ is the bacterial flux and j is the amount of fluid dragged by each bacterium. The nonlinearity in the diffusion term causes the fluid field to have a sharp boundary (singular line) at the front of the colony, as is observed in the bacterial colonies (Fig. 5).

The complete model for the bacterial colony is:

$$\begin{aligned}
\frac{\partial b}{\partial t} &= D_b \nabla \cdot (l^{-2\gamma} \nabla b) + bn - \mu b \\
\frac{\partial n}{\partial t} &= D_n \nabla^2 n - bn \\
\frac{\partial l}{\partial t} &= \nabla \cdot (D_l l^{\eta} \nabla l + j D_b l^{-2\gamma} \nabla b) \\
&\quad + \Gamma bn(l_{\max} - l) - \lambda l \\
\frac{\partial s}{\partial t} &= \mu b \,.
\end{aligned} \tag{7}$$

The second term in the equation for b represents the reproduction of the bacteria. The reproduction depends on the local amount of nutrient and it reduces this amount. The third term in the equation for b represents the process of bacterial "freezing". For the initial condition, we set n to have uniform distribution of level n_0, b to have compact support at the center, and the other fields to be zero everywhere.

Preliminary results show that the model can reproduce branching patterns, similar to the bacterial colonies (Fig. 6). At low values of absorption rate, the model exhibits dense fingers. At higher absorption rates, the model exhibits finer branches with lower fractal dimension (Fig. 7). We also obtain finer branches with lower fractal dimension if we change other parameters that effectively decrease the amount of lubrication. We can relate these conditions to high agar concentration. Comparing the fractal dimension and growth velocity of the simulations of LBm to those of CWm (Fig. 4), it seems as if the Communicating Walkers simulations are done for a narrower range of initial food concentration. Note, however, that at the lowest concentrations the patterns of the bacterial colonies are dominated by additional effects (see Sec. 5) and both models must be modified to accommodate these effects.

We can now check the effect of bacterial discreteness on the observed colonial patterns. Following Kessler and Levine,[31] we introduce the discreteness of the system into the continuous model by repressing the growth term at low bacterial densities ("half a bacterium cannot reproduce"). The growth term is multiplied by a Heaviside step function $\Theta(b-\beta)$, where β is the threshold density for growth. In Fig. 8, we show the effect of various values of β on the pattern. High cutoff values make the model more sensitive to the implicit anisotropy of the underlying tridiagonal lattice used in the simulation. The result is dendritic growth with marked six-fold

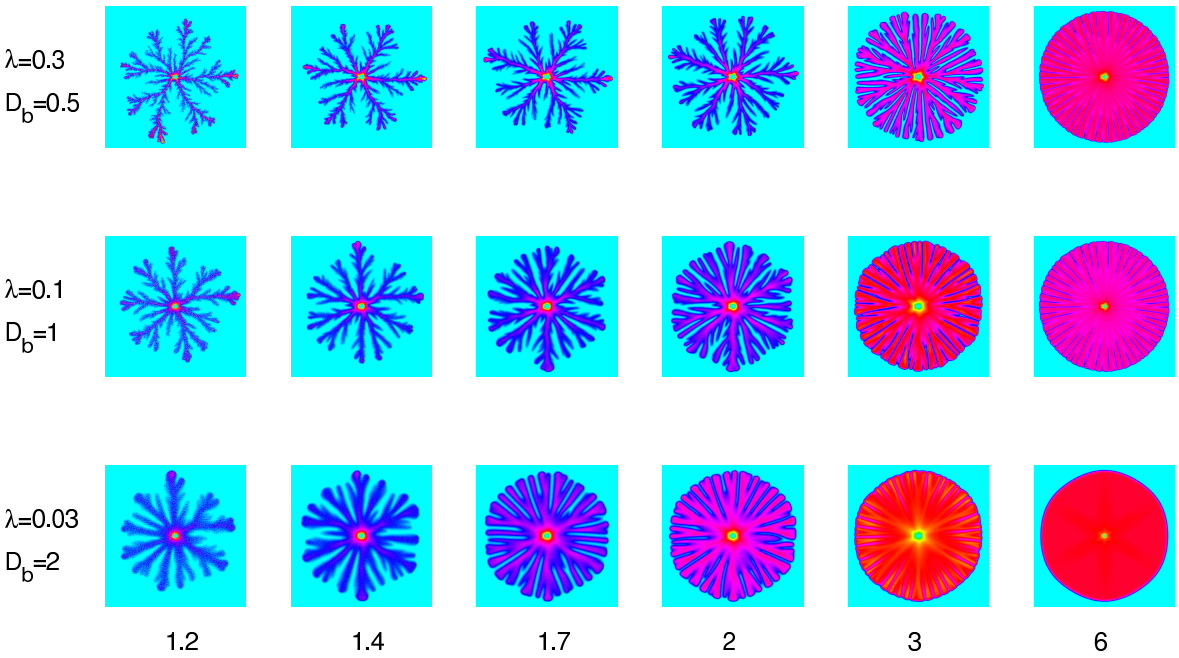

Fig. 6 Growth patterns of LBm, for different values of initial nutrient level n_0 (printed at the bottom of the columns), and different values of the parameters D_b and λ. The different sets of values for these later parameters are related to different values of agar concentration, with lowest concentration at the bottom row. The apparent (though weak) six-fold anisotropy is due to the underlying tridiagonal lattice. The different colors represent different densities of bacteria, both active and stationary, i.e. different values of $b+s$.

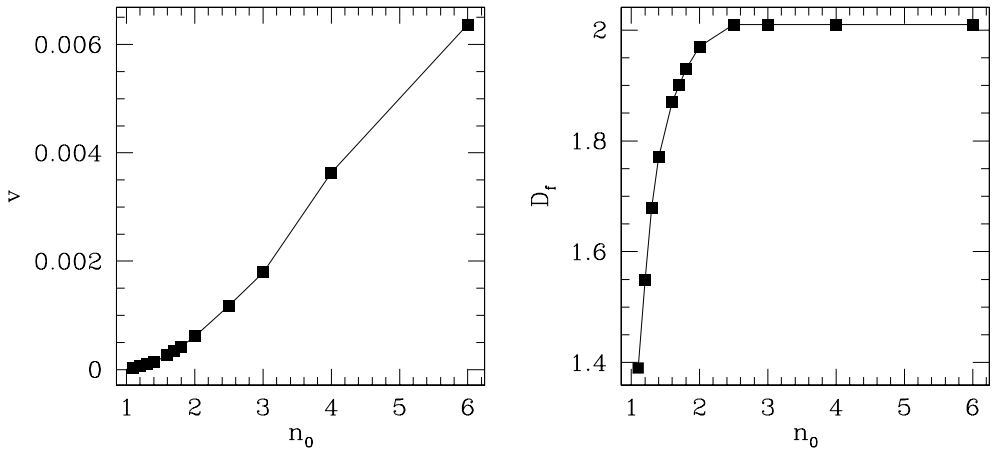

Fig. 7 Fractal dimension and growth velocity as a function of initial food concentrations. The data are for typical runs of LBm with parameters as in the middle row of Fig. 6. The growth velocity is presented in arbitrary units.

Fig. 8 The effect of a cutoff on the growth patterns in LBm. Aside from the cutoff, the conditions and parameters are the same in all patterns. In such conditions, the maximal value of b is about 0.025. The values of the cutoff β are, from left to right, 10^{-6}, 10^{-5} and $3 \cdot 10^{-5}$. The six-fold symmetry is due to anisotropy of the underlying lattice which is enhanced by the cutoff.

symmetry of the pattern. Increased values of cutoff also decrease the maximal values of b reached in the simulations (and the total area occupied by the colony).

The reason for the pattern turning dendritic is as follows: the difference between tip-splitting growth and dendritic growth is the relative strength of the effect of anisotropy and an effective surface tension.[4] In LBm, there is no explicit anisotropy and no explicit surface tension. The implicit anisotropy is related to the underlying lattice, and the effective surface tension is related to the width of the front. The cutoff prevents the growth at the outer parts of the front, thus making it thinner, reduces the effective surface tension and enables the implicit anisotropy to express itself.

We stress that it is possible to find a range of parameters in which the growth patterns resemble the bacterial patterns, in spite of a high value of cutoff. Yet the cutoff does not improve the model in any sense, it introduces an additional parameter, and it slows the numerical simulation. We believe that the well-defined boundary makes the cutoff (as a representation of the bacterial discreteness) unnecessary.

4. NON-LINEAR DIFFUSION

It is possible to introduce a simplified model, where the fluid field is not included, and is replaced by a density-dependent diffusion coefficient for the bacteria $D_b \sim b^k$.[9,38] Such a term can be justified by a few assumptions about the dynamics at low bacterial and lubrication densities:

(a) The production of lubricant is proportional to the bacterial density to the power $\alpha > 0$ ($\alpha = 1$ in the previous model).
(b) There is a sink in the equation for the time evolution of the lubrication field, e.g. absorption of the lubricant into the agar. This sink

is proportional to the lubrication density to the power $\beta > 0$ ($\beta = 1$ in the previous model).

(c) Over the bacterial length scale, the two processes above are much faster than the diffusion process, so the lubrication density is proportional to the bacterial density to the power of β/α.

(d) The friction is proportional to the lubrication density to the power $\gamma < 0$.

Given the above assumptions, the lubrication field can be removed from the dynamics and be replaced by a density-dependent diffusion coefficient. This coefficient is proportional to the bacterial density to the power $k \equiv -2\gamma\beta/\alpha > 0$.

A model of this type, the Non-Linear Diffusion model (NLDm) was offered by Kitsunezaki[15] and by Cohen:[38]

$$\frac{\partial b}{\partial t} = \nabla \cdot (D_0 b^k \nabla b) + nb - \mu b \tag{8}$$

$$\frac{\partial n}{\partial t} = \nabla^2 n - bn \tag{9}$$

$$\frac{\partial s}{\partial t} = \mu b\,. \tag{10}$$

For $k > 0$, time evolution of the model in 1-D gives rise to a front "wall", with compact support (i.e. $b = 0$ outside a finite domain). For $k > 1$, this

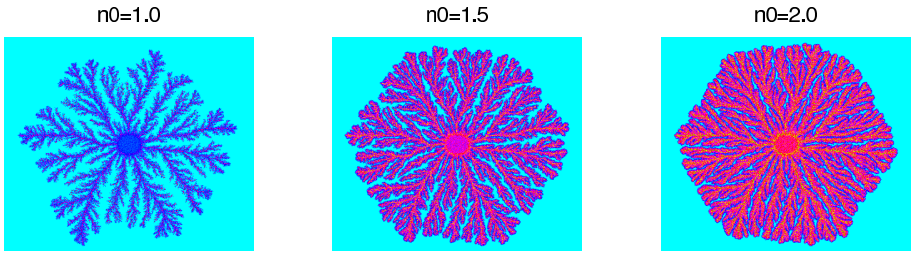

Fig. 9 Growth patterns of the NLD model, for different values of initial nutrient level n_0. Parameters are: $D_0 = 0.1, k = 1$ and $\mu = 0.15$. The apparent six-fold symmetry is due to the underlying tridiagonal lattice. The different colors represent different values of the combined field $b + s$.

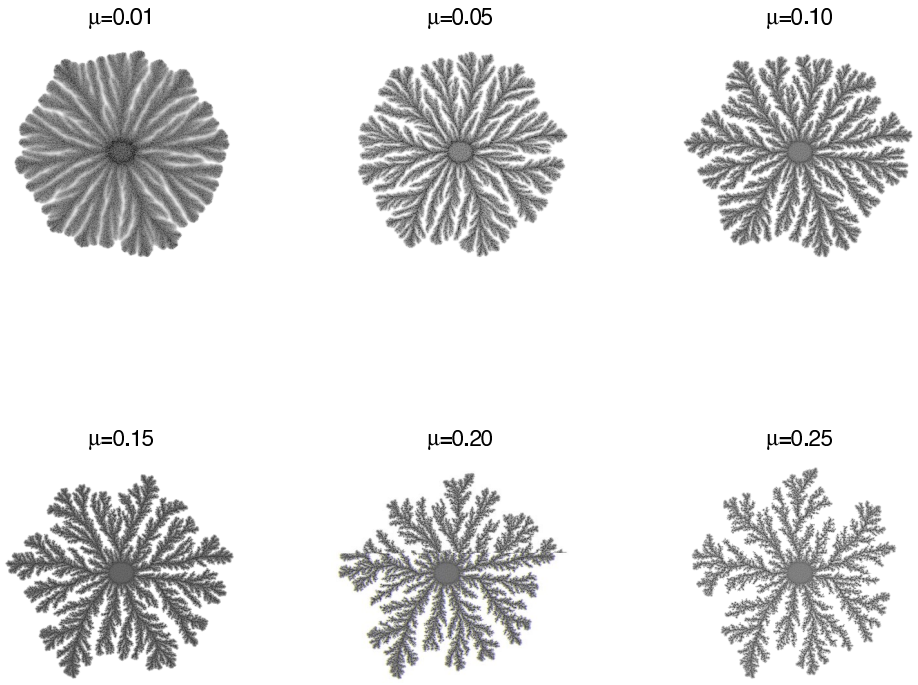

Fig. 10 Growth patterns of the NLD model, with varying values of μ. All other parameters are as in Fig. 9, left pattern. The apparent six-fold symmetry is due to the underlying tridiagonal lattice.

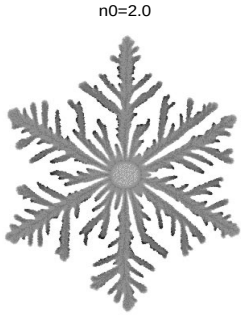

Fig. 11 Growth patterns of the NLDm, with a cutoff correction. Cutoff value $\beta = 0.1$, all other parameters as in Fig. 9, right pattern. The apparent six-fold symmetry is due to the underlying tridiagonal lattice.

wall has an infinite slope. The model exhibits branching patterns for suitable parameter values and initial conditions, as depicted in Fig. 9. Increasing the initial nutrient level makes the colonies more dense, similarly to what happens in the other models.

Changes in other parameters of the model can result in similar changes in the pattern. In Fig. 10, we present the effect of μ, the rate in which the bacteria turn stationary. Two strains of the bacteria which differ only in their corresponding values of μ can have different colonial patterns at the same growth conditions, but similar patterns in different growth conditions. In Ref. 39, we discuss the relation between variations in the model's parameters, bacterial strains and developing patterns.

As in LBm, adding the "Kessler and Levine correction" to the model, i.e. making the growth term vanish for $b < \beta$, does not seem to make the patterns "better", or closer to the experimental observations (Fig. 11). The apparent increased sensitivity to the implicit anisotropy results from the narrowed front, which decreases the effective surface tension.

5. CHEMOTAXIS

So far, we have tested the models for their ability to reproduce macroscopic patterns and microscopic dynamics of the bacterial colonies. All succeeded equally well, reproducing some aspects of the microscopic dynamics and the patterns in some range of nutrient level and agar concentration. However, the same results can be obtained with other models (Ref. 19 and references therein). We will now extend CWm and NLDm to test for their success in describing other aspects of the bacterial colonies involving chemotaxis and chemotactic signaling (which are believed to by used by the bacteria[5,35–37]). Chemotaxis means changes in the movement of the cell in response to a gradient of certain chemical field.[40–43] The movement is biased along the gradient either in the gradient direction or in the opposite direction. Usually chemotactic response means a response to an externally produced field, like in the case of chemotaxis towards food. However, the chemotactic response can also be to a field produced directly or indirectly by the bacterial cells. We will refer to this case as chemotactic signaling. The bacteria sense the local concentration r of a chemical via membrane receptors binding the chemical's molecules.[40,42] It is crucial to note that when estimating gradients of chemicals, the cells actually measure changes in the receptors' occupancy and not in the concentration itself. When put in continuous equations,[19,44] this indirect measurement translates to measuring the gradient

$$\frac{\partial}{\partial x}\frac{r}{(K+r)} = \frac{K}{(K+r)^2}\frac{\partial r}{\partial x} \tag{11}$$

where K is a constant whose value depends on the receptors' affinity, the speed in which the bacterium processes the signal from the receptor, etc. This means that the chemical gradient times a factor $K/(K+r)^2$ is measured. This factor is known as the "receptor law".[44]

When modeling chemotaxis performed by walkers, it is possible to modulate the periods between tumbling (without changing the speed) in the same way as the bacteria. It can be shown that step length modulation has the same mean effect as keeping the step length constant and biasing the direction of the steps (higher probability to move in the preferred direction). As this later approach is numerically simpler, this is the one implemented in CWm.

In a continuous model, we incorporate the effect of chemotaxis by introducing a chemotactic flux $\mathbf{J}_{\text{chem}}$:

$$\mathbf{J}_{\text{chem}} \equiv \zeta(\sigma)\chi(r)\nabla r \tag{12}$$

$\chi(r)\nabla r$ is the gradient sensed by the cell (with $\chi(r)$ having the units of 1 over chemical's concentration). $\chi(r)$ is usually taken to be either constant or the "receptor law". $\zeta(\sigma)$ is the bacterial response to the sensed gradient (having the same units as a diffusion coefficient). In NLDm, the bacterial diffusion is $D_b = D_0 b^k$, and the bacterial response to chemotaxis is $\zeta(b) = \zeta_0 b(D_0 b^k) = \zeta_0 D_0 b^{k+1}$. ζ_0 is

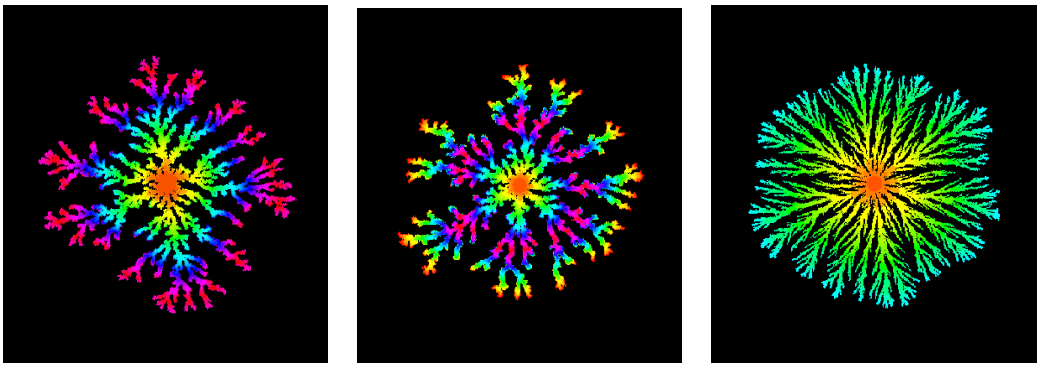

Fig. 12 The effect of chemotaxis on the growth in CWm. Growth conditions and model's parameters are the same in all patterns, excluding parameters related to chemotaxis. The different colors represent different growth times, and indicate the speed of colonial growth. In the center: a typical colony without chemotaxis. On the left: chemotaxis towards food is included in the model. The growth velocity is almost doubled, but the pattern is essentially unchanged by food chemotaxis. On the right: repulsive chemotactic signaling is included in the model. The pattern is of fine radial branches with circular envelope, like the bacterial colony presented in Fig. 1, left pattern.

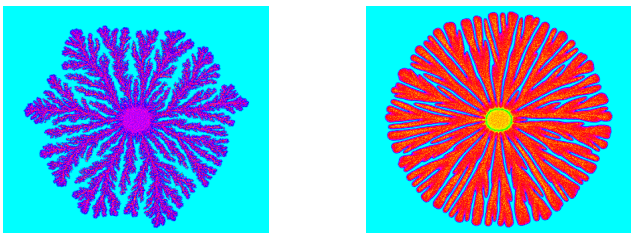

Fig. 13 Growth patterns of NLDm with food chemotaxis (left) and repulsive chemotactic signaling (right) included. For food chemotaxis $\chi_0 = 3$. For repulsive chemotactic signaling $\chi_0 = -1$, $D_r = 1$, $\Gamma_r = 0.25$, $\Omega_r = 0$ and $\Lambda_r = 0.001$. Other parameters are the same as in Fig. 9, middle pattern. The apparent six-fold symmetry is due to the underlying tridiagonal lattice.

a constant, positive for attractive chemotaxis and negative for repulsive chemotaxis.

Ben-Jacob et al. argued[5,35–37] that for the colonial adaptive self-organization, the bacteria employ three kinds of chemotactic responses, each dominant in different regimes of growth conditions. One response is the food chemotaxis mentioned above. It is expected to be dominant for an intermediate range of nutrient levels (see the "receptor law" above). The other two kinds of chemotactic responses are signaling chemotaxis. One is long-range repulsive chemotaxis; the repelling chemical is secreted by starved bacteria at the inner parts of the colony. The second signal is a short-range attractive chemotaxis (this signal will not be discussed here). The length scale of each signal is determined by the diffusion constant of the chemical agent and the rate of its spontaneous decomposition.

Amplification of Diffusive Instability Due to Nutrients Chemotaxis: In non-living systems, more ramified patterns (lower fractal dimension) are observed for lower growth velocity. Based on growth velocity as function of nutrient level and on growth dynamics, Ben-Jacob et al.[11] concluded that in the case of bacterial colonies there is a need for a mechanism that can both increase the growth velocity and maintain, or even decrease, the fractal dimension. They suggested food chemotaxis as the required mechanism. It provides an outward drift to the cellular movements; thus, it should increase the rate of envelope propagation. At the same time, being a response to an external field it should also amplify the basic diffusion instability of the nutrient field. Hence, it can support faster growth velocity together with a ramified pattern of low fractal dimension.

The above hypothesis was tested in CWm and in NLDm. In Figs. 12 and 13 it is shown that as expected, the inclusion of food chemotaxis in both models led to a considerable increase of the growth velocity without significant change in the fractal dimension of the pattern.

Repulsive chemotactic signaling: We focus now on the formation of the fine radial branching patterns at low nutrient levels. From the study of non-living systems, it is known that in the same manner that an external diffusion field leads to the diffusion instability, an internal diffusion field will stabilize the growth. It is natural to assume that some sort of chemotactic agent produces such a field. To regulate the organization of the branches, it must

be a long-range signal. To result in radial branches it must be a repulsive chemical produced by cells at the inner parts of the colony. The most probable candidates are the bacteria entering a pre-spore stage.

If nutrient is deficient for a long enough time, bacterial cells may enter a special stationary state — a state of a spore — which enables them to survive much longer without food. While the spores themselves do not emit any chemicals (as they have no metabolism), the pre-spores (sporulating cells) do not move and emit a very wide range of waste materials, some of which are unique to the sporulating cell. These emitted chemicals might be used by other cells as a signal carrying information about the conditions at the location of the pre-spores. Ben-Jacob et al.[11,36,45] suggested that such materials are repelling the bacteria ("repulsive chemotactic signaling") as if they escape a dangerous location.

The equation describing the dynamics of the chemorepellent contains terms for diffusion, production by pre-spores, decomposition by active bacteria and spontaneous decomposition:

$$\frac{\partial r}{\partial t} = D_r \nabla^2 r + \Gamma_r s - \Omega_r b r - \lambda_r r \qquad (13)$$

where D_r is the diffusion coefficient of the chemorepellent, Γ_r is the emission rate of repellent by pre-spores, Ω_r is the decomposition rate of the repellent by active bacteria, and λ_r is the rate of self-decomposition of the repellent. In CWm, b and s are replaced by active and inactive walkers, respectively.

In Figs. 12 and 13, the effect of repulsive chemotactic signaling is shown. In the presence of repulsive chemotaxis, the patterns in both models become much denser with a smooth circular envelope, while the branches are thinner and radially oriented.

6. CONCLUSIONS

We show here a pattern-forming system, bacterial colony, whose discrete elements, the bacteria, are big enough to raise the question of modeling discrete systems. We study two types of models. The CWm has explicit discrete units to represent the bacteria. The ratio between the walkers' size and the pattern's size is even bigger than the analog ratio in the bacterial colony. The second type of model is continuous reaction-diffusion equations. Nonconstant diffusion coefficient causes a sharp boundary to appear in these models. Following Kessler and Levine,[31] we account for the discreteness of the bacteria by including a cutoff in the bacterial growth term. The cutoff does not improve the models' descriptive power. The main effect of such a cutoff is to decrease the width of the colony's front, making the growth pattern more sensitive to effects such as implicit anisotropy. We conclude that the presence of a boundary cancels the need for explicit treatment of discreteness.

In order to assess the similarity between the semi-discrete CWm and the continuous NLDm, we incorporate food chemotaxis and repulsive chemotactic signaling into the models (both are expected to exist in the bacterial colonies). Both models respond to such changes in the same way, exhibiting altered patterns and altered dynamics, similar to those observed in the bacterial colonies. From this similarity, we conclude that to some extent inferences from one model can be applied to the other. Specifically, we focus on insensitivity of CWm to implicit anisotropy and on the sensitivity a cutoff imposes on the continuous models. From the two facts combined, we conclude that the magnified discreteness in the CWm is still small enough to be neglected.

Increasing number of pathogenic bacteria are developing resistance to all existing commercial antibiotics. As the bacteria develop antibiotic resistance at a higher rate than scientists develop new drugs, the deficiency in reliable anti-microbial "magic drug" becomes a severe health problem (Ref. 46 and references therein) (see also the UN's World Health Report 1996[47]). To reverse this course of events, scientists have to "outsmart" bacteria by taking new avenues of study that will lead to the development of novel therapeutic strategies to fight them. There is a growing recognition of bacterial communication and cooperation as having a major role in bacterial behavior, including pathogenicity (D. G. Davies et al.[48] are attempting to reduce the pathogenicity of *Pseudomonas aeruginosa* by interfering with intercellular communication).

Generic models like those presented here may lead to new insights into the effects of antibiotics on bacterial colonies and into cooperative resistance to antibiotics. For example, an important issue related to resistance acquisition is the effect of non-lethal concentrations of antibiotics on the bacteria. A

naive assumption would be that antibiotics simply reduce the vitality of the bacteria, causing them to die faster (or become stationary, in the case of growth-inhibiting antibiotics). This assumption can be easily tested in the model by increased values of μ. Comparison of Fig. 10 to experiments shows that the case is rarely as simple as that. Elsewhere,[49] we present a study of the effect of different antibiotics on bacterial colonies.

ACKNOWLEDGMENTS

We have benefited from many discussions on the presented studies with H. Levine. Identifications of the *Paenibacillus dendritiformis* and genetic studies are carried out in collaboration with D. Gutnick's group. Presented studies are supported in part by a grant from the Israeli Academy of Sciences grant No. 593/95, by the Israeli-US Binational Science Foundation BSF grant No. 00410-95 and by The Milo and Shoshana Shefler Project. I. Cohen wishes to thank The Colton Scholarships for their support.

REFERENCES

1. J. Kepler, *De Nive Sexangula Godfrey Tampach* (Frankfurt am Main, 1611).
2. B. B. Mandelbrot, *The Fractal Geometry of Nature* (Freeman, San Francisco, 1977).
3. T. Vicsek, *Fractal Growth Phenomena* (World Scientific, Singapore, 1989).
4. E. Ben-Jacob, "From Snowflake Formation to the Growth of Bacterial Colonies. Part I: Diffusive Patterning in Non-Living Systems," *Contemp. Phys.* **34**, 247–273 (1993).
5. E. Ben-Jacob, "From Snowflake Formation to the Growth of Bacterial Colonies. Part II: Cooperative Formation of Complex Colonial Patterns," *Contemp. Phys.* **38**, 205–241 (1997).
6. D. A. Kessler, J. Koplik and H. Levine, "Pattern Selection in Fingered Growth Phenomena," *Adv. Phys.* **37**, 255 (1988).
7. J. S. Langer, "Dendrites, Viscous Fingering, and the Theory of Pattern Formation," *Science* **243**, 1150–1154 (1989).
8. E. Ben-Jacob and P. Garik, "The Formation of Patterns in Non-Equilibrium Growth," *Nature* **343**, 523–530 (1990).
9. E. Ben-Jacob, I. Cohen and H. Levine, "Cooperative Self-Organization of Microorganisms," *Adv. Phys.* 1999 (in press).
10. M. Matsushita and H. Fujikawa, "Diffusion-Limited Growth in Bacterial Colony Formation," *Physica* **A168**, 498–506 (1990).
11. E. Ben-Jacob, O. Shochet, A. Tenenbaum, I. Cohen, A. Czirók and T. Vicsek, "Generic Modeling of Cooperative Growth Patterns in Bacterial Colonies," *Nature* **368**, 46–49 (1994).
12. E. Ben-Jacob, I. Cohen, O. Shochet, A. Czirók and T. Vicsek, "Cooperative Formation of Chiral Patterns During Growth of Bacterial Colonies," *Phys. Rev. Lett.* **75**(15), 2899–2902 (1995).
13. K. Kawasaki, A. Mochizuki, M. Matsushita, T. Umeda and N. Shigesada, "Modeling Spatio-Temporal Patterns Created by Bacillus-Subtilis," *J. Theor. Biol.* **188**, 177–185 (1997).
14. E. Ben-Jacob, I. Cohen, A. Czirók, T. Vicsek and D. L. Gutnick, "Chemomodulation of Cellular Movement and Collective Formation of Vortices by Swarming Bacteria and Colonial Development," *Physica* **A238**, 181–197 (1997).
15. S. Kitsunezaki, "Interface Dynamics for Bacterial Colony Formation," *J. Phys. Soc. Japan* **66**(5), 1544–1550 (1997).
16. M. Matsushita, J. Wakita, H. Itoh, I. Rafols, T. Matsuyama, H. Sakaguchi and M. Mimura, "Interface Growth and Pattern Formation in Bacterial Colonies," *Physica* **A249**, 517–524 (1998).
17. I. Rafols, *Formation of Concentric Rings in Bacterial Colonies*, M. Sc. Thesis, Chuo University, Japan (1998).
18. Y. Kozlovsky, I. Cohen, I. Golding and E. Ben-Jacob, "Lubricating Bacteria Model for Branching Growth of Bacterial Colonies," *Phys. Rev.* **E59**, 7025–7035 (1999).
19. I. Golding, Y. Kozlovsky, I. Cohen and E. Ben-Jacob, "Studies of Bacterial Branching Growth Using Reaction-Diffusion Models of Colonial Development," *Physica* **A260**(3–4), 510–554 (1998).
20. S. E. Esipov and J. A. shapiro, "Kinetic Model of *Proteus Mirabilis* Swarm Colony Development," *J. Math. Biol.* **36**, 249–268 (1998).
21. N. H. Mendelson and J. Lega, "A Complex Pattern of Traveling Stripes is Produced by Swimming Cells of *Bacillus Subtilis*," *J. Bacteriol.* **180**, 3285–3294 (1998).
22. N. H. Mendelson, A. Bourque, K. Wilkening, K. R. Anderson and J. C. Watkins, "Organized Cell Swimming Motions in *Bacillus Subtilis* Colonies: Patterns of Short-Lived Whirls and Jets," *J. Bacteriol.* **181**, 600–609 (1999).
23. E. Ben-Jacob, H. Shmueli, O. Shochet and A. Tenenbaum, "Adaptive Self-organization During Growth of Bacterial Colonies," *Physica* **A187**, 378–424 (1992).
24. E. Ben-Jacob, A. Tenenbaum, O. Shochet and O. Avidan, "Holotransformations of Bacterial

Colonies and Genome Cybernetics," *Physica* **A202**, 1–47 (1994).
25. M. Tcherpikov, E. Ben-Jacob and D. Gutnick, *Paenibacillus Dendritiformis* sp. nov., Proposal for a New Pattern-Forming Species and its Localization Within a Phylogenetic Cluster," *Int. J. Syst. Bacteriol.* **49**, 239–246 (1999).
26. H. Fujikawa and M. Matsushita, "Fractal Growth of *Bacillus Subtilis* on Agar Plates," *J. Phys. Soc. Japan* **58**, 3875–3878 (1989).
27. T. Matsuyama, K. Kaneda, Y. Nakagawa, K. Isa, H. Hara-Hotta and I. Yano, "A Novel Extracellular Cyclic Lipopeptide which Promotes Flagellum-Dependent and Independent Spreading Growth of *Serratia Marcescens*," *J. Bacteriol.* **174**, 1769–1776 (1992).
28. T. Matsuyama and M. Matsushita, "Morphogenesis by Bacterial Cells," in *Fractal Geometry in Biological Systems, An Analytical Approach*, eds. P. M. Iannaccone and M. K. Khokha (CRC Press, New York, 1995), pp. 127–171.
29. N. H. Mendelson and B. Salhi, "Patterns of Reporter Gene Expression in the Phase Diagram of *Bacillus Subtilis* Colony Forms," *J. Bacteriol.* **178**, 1980–1989 (1996).
30. J. Wakita, I. Rafols, H. Itoh, T. Matsuyama and M. Matsushita, "Experimental Investigation on the Formation of Dense-Branching-Morphology-Like Colonies in Bacteria," *J. Phys. Soc. Japan* **67**, 3630–3636 (1998).
31. D. A. Kessler and H. Levine, "Fluctuation-Induced Diffusive Instabilities," *Nature* **394**, 556–558 (1998).
32. O. Shochet, K. Kassner, E. Ben-Jacob, S. G. Lipson and H. Müller-Krumbhaar, "Morphology Transition During Non-Equilibrium Growth: I. Study of Equilibrium Shapes and Properties," *Physica* **A181**, 136–155 (1992).
33. O. Shochet, K. Kassner, E. Ben-Jacob, S. G. Lipson and H. Müller-Krumbhaar, "Morphology Transition during Non-Equilibrium Growth: II. Morphology Diagram and Characterization of the Transition," *Physica* **A187**, 87–111 (1992).
34. O. Shochet, *Study of Late-Stage Growth and Morphology Selection During Diffusive Patterning*," Ph.D. Thesis, Tel-Aviv University (1995).
35. E. Ben-Jacob, I. Cohen and A. Czirók, "Smart Bacterial Colonies," in *Physics of Biological Systems: From Molecules to Species*, Lecture Notes in Physics (Springer-Verlag, Berlin, 1997) pp. 307–324.
36. I. Cohen, A. Czirók and E. Ben-Jacob, "Chemotactic-Based Adaptive Self Organization During Colonial Development," *Physica* **A233**, 678–698 (1996).
37. E. Ben-Jacob and I. Cohen, "Cooperative Formation of Bacterial Patterns," in *Bacteria as Multicellular Organisms*, eds. J. A. Shapiro and M. Dworkin (Oxford University Press, New York, 1997).
38. I. Cohen, *Mathematical Modeling and Analysis of Pattern Formation and Colonial Organization in Bacterial Colonies*, M.Sc. Thesis, Tel-Aviv University, Israel (1997).
39. I. Golding, I. Cohen and E. Ben-Jacob, "Spatio-Selection in Expanding Bacterial Colonies," submitted to *Europhys. Lett.* (1999).
40. J. Adler, "Chemoreceptors in Bacteria," *Science* **166**, 1588–1597 (1969).
41. H. C. Berg and E. M. Purcell, "Physics of Chemoreception," *Biophysical Journal* **20**, 193–219 (1977).
42. J. M. Lackiie, ed. *Biology of the chemotactic response* (Cambridge University Press, 1986).
43. H. C. Berg, *Random Walks in Biology* (Princeton University Press, Princeton, N.J., 1993).
44. J. D. Murray, *Mathematical Biology* (Springer-Verlag, Berlin, 1989).
45. E. Ben-Jacob, O. Shochet, A. Tenenbaum, I. Cohen, A. Czirók and T. Vicsek, "Communication, Regulation and Control During Complex Patterning of Bacterial Colonies," *Fractals* **2**(1), 15–44 (1994).
46. C. F. Amáblie-Cueva, M. Cárdenas-García and M. Ludgar, "Antibiotic Resistance," *Am. Sci.* **83**, 320–329 (1995).
47. World Health Organization, Report of The Director-General, *The World Health Report 1996: Fighting Disease, Fostering Development*, Geneva (1996).
48. D. G. Davies, M. R. Parsek, J. P. Pearson, B. H. Iglewski, J. W. Costerton and E. P. Greenberg "The Involvement of Cell-to-Cell Signals in the Development of a Bacterial Biofilm," *Science* **280**, 295–298 (1998).
49. I. Cohen, E. Ben-Jacob, I. Golding and I. G. Ron, *The Effect of Antibiotic on Cooperative Bacterial Patterning*, 1999 (in preparation).